Mechanism of Sulfide-Quinone Reductase Investigated Using Site-Directed Mutagenesis and Sulfur Analysis[†,‡]

Christoph Griesbeck, Michael Schütz,[§] Thomas Schödl, Stephan Bathe, Lydia Nausch, Nicola Mederer, Martin Vielreicher, and Günter Hauska*

Lehrstuhl für Zellbiologie und Pflanzenphysiologie, Universität Regensburg, Universitätsstrasse 31, 93053 Regensburg, Germany

Received April 26, 2002; Revised Manuscript Received August 6, 2002

ABSTRACT: Biological sulfide oxidation is a reaction occurring in all three domains of life. One enzyme responsible for this reaction in many bacteria has been identified as sulfide:quinone oxidoreductase (SQR). The enzyme from *Rhodobacter capsulatus* is a peripherically membrane-bound flavoprotein with a molecular mass of approximately 48 kDa, presumably acting as a homodimer. In this work, SQR from *Rb. capsulatus* has been modified with an N-terminal His tag and heterologously expressed in and purified from *Escherichia coli*. Three cysteine residues have been shown to be essential for the reductive half-reaction by site-directed mutagenesis. The catalytic activity has been nearly completely abolished after mutation of each of the cysteines to serine. A decrease in fluorescence on reduction by sulfide as observed for the wild-type enzyme has not been observed for any of the mutated enzymes. Mutation of a conserved valine residue to aspartate within the third flavin-binding domain led to a drastically reduced substrate affinity, for both sulfide and quinone. Two conserved histidine residues have been mutated individually to alanine. Both of the resulting enzymes exhibited a shift in the pH dependence of the SQR reaction. Polysulfide has been identified as a primary reaction product using spectroscopic and chromatographic methods. On the basis of these data, reaction mechanisms for sulfide-dependent reduction and quinone-dependent oxidation of the enzyme and for the formation of polysulfide are proposed.

Inorganic reduced sulfur compounds can serve as electron donors in many phototrophic and chemotrophic bacteria, mostly with sulfate being the major oxidation product (*1*). The purple "non-sulfur" bacterium *Rhodobacter capsulatus* appears to convert sulfide exclusively into extracellular elemental sulfur S^0, however (*2*). For the initial step of the oxidation of sulfide to elemental sulfur, mainly two enzymatic systems are discussed, flavocytochrome *c* (FCC)[1] and sulfide-quinone reductase (SQR). FCC is a redox protein located in the periplasm of several species (*3*). Due to sulfide:cytochrome *c* oxidoreductase activity in vitro, FCC is suggested to play an essential role in sulfide oxidation in vivo. It consists of a FAD-binding subunit and a cytochrome *c* subunit. The enzyme is well-studied with respect to its catalytic mechanism (*4*−*8*), and the three-dimensional structure of FCC from *Allochromatium vinosum* has been determined to a resolution of 2.53 Å (*9*, *10*). Although the enzyme was found in a variety of chemotrophic and phototrophic sulfide-oxidizing bacteria, it is not obligatory in sulfide oxidation. FCC does not occur in a variety of sulfide-oxidizing bacteria, and the enzyme seems to be confined to species that are also able to oxidize thiosulfate (*1*, *3*). Moreover, mutational inactivation of FCC did not have any significant effect on the sulfide oxidizing ability of the phototrophic sulfur bacterium *A. vinosum* (*11*).

A second sulfide-oxidizing system identified in a variety of phototrophic bacteria has turned out to be a sulfide-quinone reductase (SQR). Meanwhile, sulfide oxidation by SQR and participation of the *bc* complex in sulfide-dependent electron transfer have been established in a number of phototrophic and chemotrophic bacteria (for a comprehensive review on SQR, see ref *12*). The SQR protein consists of ∼430 amino acids and has a molecular mass of nearly 50 kDa. It is peripherically bound to the membrane and can be solubilized by detergents as well as by NaBr. A non-covalently bound FAD has been shown to be the only cofactor. Fluorescence excitation and emission spectra resemble those of other flavoproteins, exhibiting excitation maxima at ∼280, ∼375, and ∼450 nm and an emission maximum at ∼520 nm. On addition of sulfide, the fluorescence reversibly drops. By C-terminal fusion with the alkaline phosphatase from *Escherichia coli*, it has been demonstrated that SQR is localized in the periplasm of *Rb. capsulatus* (*13*). Remarkably, it was shown by deletion of the *sqr* gene that SQR is essential for sulfide oxidation in *Rb. capsulatus*.

[†] This work was supported by the Deutsche Forschungsgemeinschaft (DFG).

[‡] Dedicated to Horst Kisch on the occasion of his 60th birthday.

* To whom correspondence should be addressed: Lehrstuhl für Zellbiologie und Pflanzenphysiologie, Universität Regensburg, Universitätsstrasse 31, 93053 Regensburg, Germany. Telephone: (49) 941 943 3031. Fax: (49) 941 943 3352. E-mail: Guenther.Hauska@biologie.uni-regensburg.de.

[§] Present address: PROFOS AG, Josef-Engert-Strasse 9, 93053 Regensburg, Germany.

[1] Abbreviations: dUQ, decylubiquinone; FCC, flavocytochrome *c*; His-SQR, SQR with a His tag and an enterokinase cleavage site at the N-terminus; SQR, sulfide-quinone reductase; units, micromoles of decylubiquinone reduced per minute.

10.1021/bi026032b CCC: $22.00
Published on Web 09/07/2002

Comparison of the amino acid sequences of SQRs with those of other flavoproteins revealed affiliation of this enzyme to the disulfide oxidoreductase flavoproteins, also named the glutathione reductase family after the most prominent member. Besides glutathione reductase FCC, lipoamide dehydrogenase, thioredoxin reductase, and mercuric ion reductase are members of this protein family (*14*). Since these enzymes catalyze electron transfer between sulfur centers (dithiol−disulfide) and carbon centers [mostly NAD(P)H−NAD(P)$^+$], they are also termed C-S-transhydrogenases (*15*). Characteristics of this family are the homodimeric organization with one FAD per subunit and a redox active disulfide bridge close to the FAD (*14*). During the reaction cycle, a covalent adduct between one of the cysteines and the C(4a) atom of FAD and a charge transfer complex with the cysteine thiolate as the donor and the oxidized FAD as the acceptor can be observed. Hereby, the thiolate form of the cysteine is stabilized by base catalysis. This interaction seems to be conserved within the glutathione reductase family. Sequence homology between SQR and this family can be observed mainly within three FAD-binding domains. Apart from the FAD-binding domains, there are six highly conserved regions within the SQR sequence, which are specific for SQR and can therefore be considered as SQR fingerprint regions (*12*).

Sulfide oxidation is not confined to prokaryotes. Coupling of ATP synthesis to sulfide oxidation is known for different groups of eukaryotes such as annelides, molluscs, and vertebrates (*16*, *17*). Recently, sulfide oxidation could be observed in mitochondria of tissues from organisms that are not specially adapted to sulfide-rich environments such as chicken liver (*18*) and the colonic mucosa of rats (*19*). A gene encoding a protein with sulfide-quinone reductase activity has been identified in fission yeast (*20*). However, the K_m values of 2 mM for the binding of sulfide and quinone by HMT2 are nearly 1000 times higher than the K_m values of all characterized SQR proteins (*12*). In addition, the SQR fingerprint regions are not conserved in HMT2.

At present, no data about the catalytic mechanism of sulfide oxidation by SQR are available. In this work, site-directed mutagenesis on SQR has been carried out in an effort to elucidate specific functions of several conserved amino acids. In addition, the sulfur product of the SQR reaction has been investigated. Taken together and in comparison to the well-studied mechanisms of other members of the glutathione reductase family, a reaction model for the sulfide-dependent reduction of SQR, the formation of the sulfur product, and the quinone-dependent reoxidation of the enzyme is presented.

MATERIALS AND METHODS

Bacterial Strains. All cloning steps were performed using *E. coli* strain DH10B (*21*). Heterologous expression of SQR in *E. coli* was carried out in BL21(DE3) cells (*22*). For site-directed mutagenesis, *E. coli* strains JM109 and BMH 71-18 from Promega (Madison, WI) were used. Conjugation was performed with *E. coli* HB101 (*23*). *Rb. capsulatus* wild-type strain DSMZ 155 was obtained from the Deutsche Sammlung von Mikroorganismen und Zellkulturen. The construction of the *sqr*$^-$ strain F14 was described previously (*13*). *Rb. capsulatus* was cultured under photosynthetic conditions (*13*).

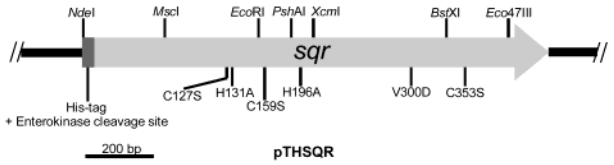

FIGURE 1: Cloning of the mutations into pTHSQR. The positions of the mutations and the restriction sites are shown.

DNA Manipulations and Plasmids. Methods for DNA manipulation were standard (*23*). Oligonucleotides were obtained from MWG-Biotech (Ebersberg, Germany).

Construction of the Expression Plasmid pTHSQR. pTHSQR was obtained by addition of the codons for amino acids MHHHHHHDDDDK to the 5′-end of the *sqr* gene, leading to an N-terminal modification consisting of a His tag and the cleavage site for the protease enterokinase. PCR was performed using the primers pMalHis6-SQR (AAA CAT ATG CAT CAC CAT CAC CAT CAC GAT GAC GAT GAC AAA GCT CAT ATC GTG GTT CTG GGC GCC GG) and sqr187 (GCC CGA CAT AGG GTT CCG) and the plasmid pUSQR (*24*) as a template. The resulting PCR product was cut with the restriction enzymes *Nde*I and *Eco*RI (Figure 1) and ligated into the *Nde*I−*Eco*RI site of the plasmid pTSQR (*24*), a derivative of pT7-7 (*25*). The resulting modified *sqr* gene was controlled by DNA sequencing.

Site-Directed Mutagenesis. Site-directed mutagenesis was carried out using the GeneEditor kit from Promega and the plasmid pTHSQR. The mutations were constructed using the corresponding oligonucleotides given in parentheses: C127S (CAG TCG ATC **A**GC CAT ATC GA), H131A (CG ATC TGC CAT ATC GAC **GCG** GCC GAG GCG GCA GGA G), C159S (GGC GCC AGC **A**GC TTC GGC CC), H196A (CG GAA CCC TAT GTC GGG **GCG** CTG GGG CTG GAC GGG), V300D (C GCG GTG GGG G**A**C TGC GTG GCG), and C353S (AAC GCC GTC T**C**T CTG GCG GA). The bases deviating from the original sequence are shown in bold letters. Fragments containing the individual mutations were cut and cloned into the identically cut original plasmid pTHSQR to minimize the risk of additional mutations. For the different mutations, the following combinations of restriction enzymes as shown in Figure 1 were used: *Msc*I and *Psh*AI for C127S, H131A, and C159S, *Psh*AI and *Bst*XI for H196A, *Xcm*I and *Bst*XI for V300D, and *Bst*XI and *Eco*47III for C353S. The resulting mutated *sqr* genes were controlled by DNA sequencing.

Conjugation Techniques. For conjugation, the plasmids pPSQR and pPSQR′ containing one of the single mutations within the *sqr* gene were mobilized into *Rb. capsulatus* using triparental mating (*13*).

Heterologous Expression and Purification of His-SQR. Wild-type SQR or mutated SQRs were purified from 2 L cultures of *E. coli* BL21(DE3) harboring the plasmid pTHSQR or pTHSQR′ containing one of the point mutations, respectively. Expression was induced at an A_{600} of 0.8−1.0 by adding 1 mM isopropyl 1-thio-β-D-galactopyranoside (IPTG-b, biological grade) (Gerbu Biotechnik, Gaiberg, Germany) for 8 h at 25 °C. Cells were harvested and washed with 200 mL of buffer containing 50 mM Bis-Tris (pH 6.5) and 2 mM $MgCl_2$. After centrifugation, cells were resuspended in 20 mL of the same buffer, homogenized by

Table 1: Results of Site-Directed Mutagenesis in Comparison to the Properties of Wild-Type (wt) SQR[a]

	wt	C127S	C159S	C353S	V300D	H131A	H196A
complementation[b]	+	−	−	−	nd	nd	nd
specific activity[c]	50−55	0.74	0.27	0.23	6	11 (pH 6.5) 15 (pH 4.5)	21 (pH 6.5) 22 (pH 6.2)
activity as a percentage of that of the wild type (%)	100	1.3	0.5	0.4	11	20 (pH 6.5) 27 (pH 4.5)	38 (pH 6.5) 40 (pH 6.2)
K_M for sulfide (μM)	5	3	/	/	>400	11	15
K_M for decylubiquinone (μM)	3	nd	/	/	>28	4	3
pH optimum	6.7	nd	/	/	nd	4.5	6.2
fluorescence quenched by sulfide	+	−	−	−	+	+	+
reoxidation by decylubiquinone	+	/	/	/	+	−	+

[a] +, positive; −, negative; /, not measurable; nd, not determined. [b] Complementation of *Rb. capsulatus* F14 (*sqr*$^-$), growth on sulfide. [c] Specific activity (micromoles of decylubiquinone per milligram of protein per minute) at pH 6.5 and at the pH optimum.

pottering, and broken by French press treatment (12 000 psi). After low-speed centrifugation (7000*g* for 20 min), the membranes were collected by ultracentrifugation (1 h at 200000*g*), washed in the same buffer, and resuspended in 20 mL of 50 mM Bis-Tris (pH 6.5). For solubilization, Thesit (Boehringer Mannheim, Mannheim, Germany) was added to a final concentration of 0.6%. After being stirred on ice in darkness for 1 h, the sample was centrifuged (200000*g* for 1 h). The supernatant was mixed with Ni-bound NTA (Qiagen, Hilden, Germany), shaken for 1 h at 6 °C, and packed into a column. The column was first washed with buffer containing 50 mM Bis-Tris (pH 6.5), 300 mM NaCl, 10% glycerol, and 0.025% Thesit, and subsequently with buffer containing 50 mM sodium phosphate (pH 6.0), 300 mM NaCl, 10% glycerol, and 0.025% Thesit. Then washing was carried out with 0.05 M imidazole in the same buffer. For elution, the imidazole concentration was increased up to 0.4 M. Fractions were tested by SDS−PAGE, and the SQR-containing pure fractions were collected and dialyzed against 50 mM Bis-Tris (pH 6.5) and 0.025% Thesit. Samples were concentrated using Pall Filtron Macrosep 50 K (Pall Filtron, Northborough, MA) or a Vivaspin 50000 MWCO (Vivascience, Göttingen, Germany).

SQR Activity Assay. SQR activity was determined as sulfide-dependent decylubiquinone (dUQ) reduction in a Specord S-100 B diode array spectrophotometer (Analytic Jena, Jena, Germany) recording the absorption at 275 nm − 300 nm (*26*) under an N_2 atmosphere. The millimolar differential extinction coefficient was determined by the measurement of difference spectra of oxidized and reduced dUQ to be 12.5 mM^{-1} cm^{-1} on basis of the extinction coefficient of oxidized dUQ in ethanol (ϵ_{275}) of 15 mM^{-1} cm^{-1} (*27*). The reaction mixture contained 50 mM Bis-Tris (pH 6.5), 20 mM glucose, 1 unit of glucose oxidase/mL, approximately 10 units of catalase/mL, and 40 μM dUQ. The reaction was started by addition of 40 μM Na_2S.

SDS−PAGE. SDS−polyacrylamide gel electrophoresis was carried out according to ref *28* and the gel stained with silver (ICN Rapid-Ag Stain, ICN, Irving, TX) or Coomassie.

Determination of Protein Concentrations. Protein concentrations were determined with a BCA protein assay kit (Pierce, Rockford, IL).

Determination of the Flavin Content of SQR. Absorption spectra of the purified SQR were recorded for the oxidized form and after reduction with dithionite. From the difference spectrum, the FAD content was calculated using the following extinction coefficients: $\epsilon_{450} = 11$ mM^{-1} cm^{-1} for the oxidized enzyme and $\epsilon_{450} = 1$ mM^{-1} cm^{-1} for the reduced form [which were determined for other flavoproteins of the glutathione reductase family (*14*)].

Table 2: Protein-Bound Radioactivity after the SQR Reaction at pH 8.0[a]

sample		protein μg	protein pmol	dUQ (pmol)	$Na_2{}^{35}S$ kBq	$Na_2{}^{35}S$ pmol	radioactivity in flowthrough (%)
1	SQR	22	450	5000	2	216	3.7
2	SQR	22	450	5000	3.6	400	3.7
3	SQR	22	450	5000	7.2	800	4.9
4	SQR	22	450	5000	18	2000	5.0
5	SQR	22	450	0	18	2000	4.4
6	SQR	22	450	500	18	2000	3.2
7	−	−	−	5000	18	2000	3.3
8	BSA	22	330	5000	18	2000	4.1

[a] The proportion of radioactivity in the flowthrough of the molecular sieve column is given. The overall volume was 100 μL.

Fluorescence Spectroscopy. Fluorescence spectra were recorded in a Shimadzu RF-5301 PC spectrofluorimeter (Shimadzu, Japan) under aerobic conditions.

Sulfur Analysis. Determination of sulfide concentrations was carried out according to the method of Trüper and Schlegel (*29*). HPLC analysis of sulfur compounds was performed as described by Rethmeier et al. (*30*). Elemental sulfur was extracted from a 50 μL aliquot of the sample with 50 μL of chloroform and analyzed by HPLC. Sulfate was analyzed in the aqueous phase of the chloroform extraction.

Use of $Na_2{}^{35}S$ as a Substrate for SQR. For the measurement of the amount of protein-bound radioactivity, 450 pmol of SQR was incubated with different amounts of dUQ and $Na_2{}^{35}S$ (Table 2) in a volume of 100 μL and in the presence of 250 mM Tris-HCl (pH 8.0). In control experiments, BSA was used instead of SQR or protein was omitted. The reaction was started by addition of sulfide. After 1 min, an aliquot was taken from the sample for measurement in the scintillation counter. The remaining sample was applied to a Sephadex molecular sieve column. After separation of the low-molecular weight compounds, radioactivity was quantified in the scintillation counter. An aliquot was subjected to SDS−PAGE omitting the thiol reagent 2-mercaptoethanol. The presence of radioactivity within the protein band was determined by autoradiography. For detection of radioactive elemental sulfur after the SQR reaction, the experiments were performed as described above, but in an overall volume of 500 μL. After the reaction, an aliquot was taken for scintillation counting. The remaining sample was subjected to chloroform extraction. After separation of the phases, chloroform was removed from the chloroform phase by

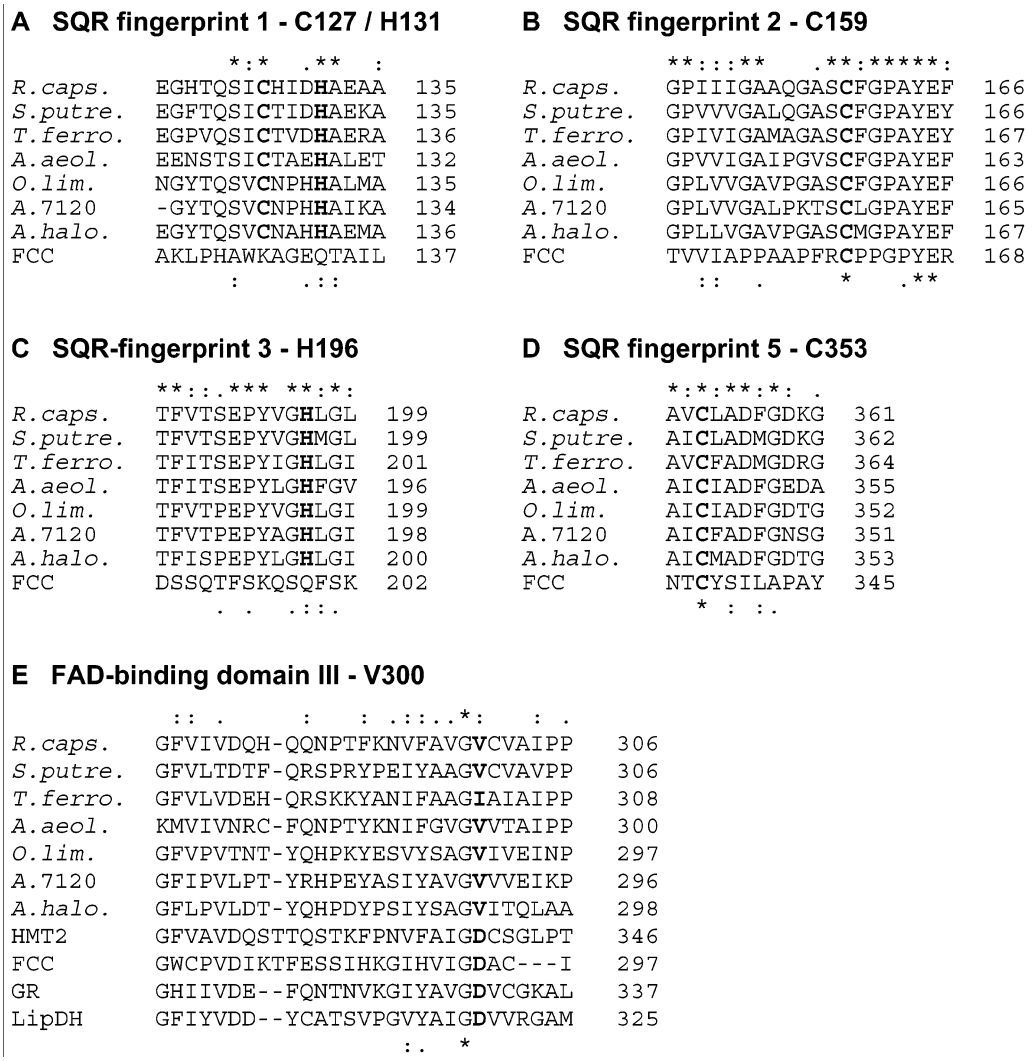

FIGURE 2: Alignments of the conserved SQR regions, including the amino acid residues chosen for mutagenesis. SQR sequences are from *Rb. capsulatus* [R.caps. (*13*)], *Shewanella putrefaciens* [S.putre. (*47*)], *T. ferrooxidans* [T.ferro. (*48*)], *Aquifex aeolicus* [A.aeol. (*49*)], *Oscillatoria limnetica* [O.lim. (*47*)], *Anabaena* ATCC 7120 [A.7120 (Kazusa DNA Research Institute)], *Aphanothece halophytica* [A.halo. (*47*)], FCC from *A. vinosum* (*10*), HMT2 from *S. pombe* (*20*), GR [human glutathione reductase (*50*)], and LipDH [lipoamide dehydrogenase from *Azotobacter vinelandii* (*51*)]. Positions of identical amino acid residues are marked with asterisks and positions of similar amino acid residues with colons (high degree of similarity) and with dots (lower degree of similarity). These positions for the SQR sequences are given above the alignment and for all shown sequences below the alignment.

evaporation, and the amount of radioactivity was determined in both phases by scintillation counting.

RESULTS

Heterologous Expression and Purification of His-SQR

The *sqr* gene from *Rb. capsulatus* has been heterologously expressed in and purified from *E. coli* (*24*). To simplify the purification process and to increase the amount of purified SQR, the gene has been fused with the codons of six histidines at the 5′-end. Cleavage of the N-terminal modification should have been achieved by introduction of the cleavage site for the protease enterokinase (Asp_4-Lys). Heterologous expression and preparation of membranes were carried out as described in Materials and Methods. After solubilization, the enzyme was purified using nickel−NTA affinity chromatography. The yield was ~3−5 mg of purified protein out of a 1 L culture of *E. coli*. Removal of the His tag by cleavage with enterokinase was attempted in solution and with the His-tagged SQR (His-SQR) bound to the nickel column. In both cases, cleavage was not achieved. Therefore, the properties of His-SQR have been compared with those of native SQR.

Properties of His-SQR

All tested properties were similar to those of the native SQR (*24*). The specific activity of 50−55 units/mg was considerably higher, however, probably due to the milder conditions of the purification protocol. The pH optimum was shifted from 6.3 to 6.7 (Figure 6), which could be a result of the N-terminal modification. The K_m values for sulfide and dUQ were 5 and 3 μM, respectively, and were on the same order of magnitude as the values for the native enzyme with 2 μM for both substrates. Both the fluorescence excitation spectrum and the emission spectrum resembled completely those of the native enzyme, exhibiting excitation maxima at ~375 and ~450 nm and an emission maximum at 520 nm (Figure 4). Upon addition of sulfide, the fluorescence dropped, and reoxidation was achieved by addition of equimolar amounts of dUQ. If an extinction coefficient for the absorption maximum around 450 nm of

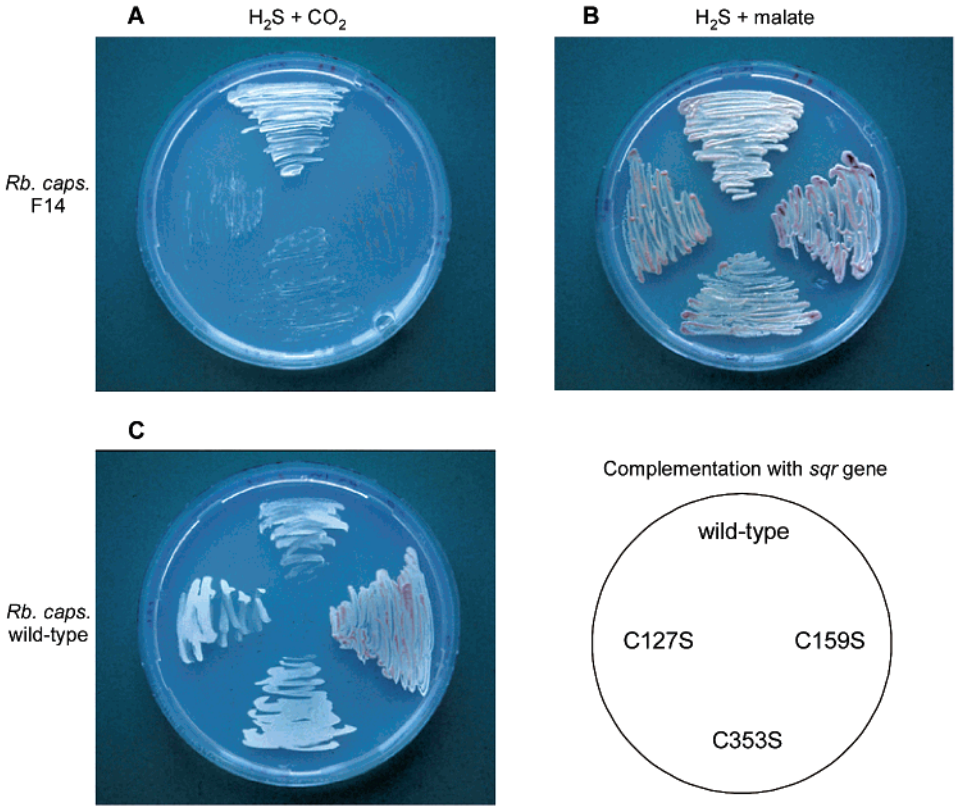

FIGURE 3: Growth of *Rb. capsulatus* with the mutated *sqr* genes and with the *sqr* wild-type (wt) gene. Strains grew for 1 week as described in Materials and Methods: (A and B) *Rb. capsulatus* strain F14 [*sqr*$^-$ (*13*)] and (C) wild-type *Rb. capsulatus*. In panels A and C, sulfide was the sole electron donor; in panel B, growth was carried out on sulfide and malate. Strains owning a functional *sqr* gene exhibit a yellowish-white coating consisting of elemental sulfur, in contrast to the red color of strains with a defective *sqr* gene. Traces of cells visible in panel A are due to thick plating of the cultures.

ca. 11 mM^{-1} cm^{-1} has been assumed for the oxidized enzyme, which has been determined for other flavoproteins of the glutathione reductase family (*14*), the absorption spectrum revealed that only 50−60% of the SQR protein monomer contained FAD (data not shown). This low content may be due to incomplete binding of flavin in the heterologous expression system or loss during purification, a phenomenon which has also been observed for other heterologously expressed flavoproteins (*20*).

Site-Directed Mutagenesis

C127S, C159S, and C353S. In flavoproteins of the disulfide oxidoreductase family, a pair of cysteines plays an important role during catalysis. While one of the cysteines interacts with a substrate thiol, the other one is responsible for the interaction with the flavin (*14*). In SQR, three cysteines each located in an SQR fingerprint region are conserved among all known sequences (Figure 2). Two of them, C159 and C353 in *Rb. capsulatus*, are also present in the related sequence of the flavoprotein subunit of flavocytochrome *c* of *A. vinosum*, forming there a redox active disulfide bridge close to the flavin moiety (*9*). The third cysteine, C127 in the *Rb. capsulatus* sequence, is not present in FCC. Each of the cysteines has been mutated to serine individually.

As a first test for investigating the importance of the cysteines for the activity of the enzyme, the plasmid pPSQR (*13*) containing one of the mutated *sqr* genes or the wild-type gene has been introduced into the *sqr*$^-$ mutant *Rb. capsulatus* F14, which has a deletion in the *sqr* gene and is therefore not able to grow on sulfide as the sole electron source (*13*). In Figure 3A, it is demonstrated that none of the three *sqr* genes with C−S exchanges could restore growth on sulfide, while the wild-type gene could do so. In the presence of sulfide and malate, growth of all strains was observed (Figure 3B). The color of the colonies with the mutated *sqr* genes was purple and appeared to be pale compared to the bright, white-yellow color of strains with an intact *sqr* gene. The pale yellow coating is due to the deposition of elemental sulfur outside the cells. This has been confirmed by HPLC analysis, as described below. Introduction of the vector carrying wild-type or mutated *sqr* genes into the *Rb. capsulatus* wild-type strain did not affect growth (Figure 3C).

The mutated His-SQRs have been expressed in and purified from *E. coli* BL21(DE3) as described for the wild-type enzyme. The activity of the purified mutated enzymes was reduced drastically to 1.3, 0.5, and 0.4% of that of the wild-type enzyme for C127S, C159S, and C353S, respectively (Table 1). In the case of C127S, the K_m value for sulfide could be determined. The resulting value of 3 μM was close to the value of 5 μM measured for the wild-type enzyme. For C159S and C353S, the activity was too low to determine K_m values.

Fluorescence excitation and emission spectra of all three mutated enzymes were identical to the wild-type spectra in the range above 300 nm, indicating incorporation of the prosthetic group FAD into the enzyme (Figure 4). However,

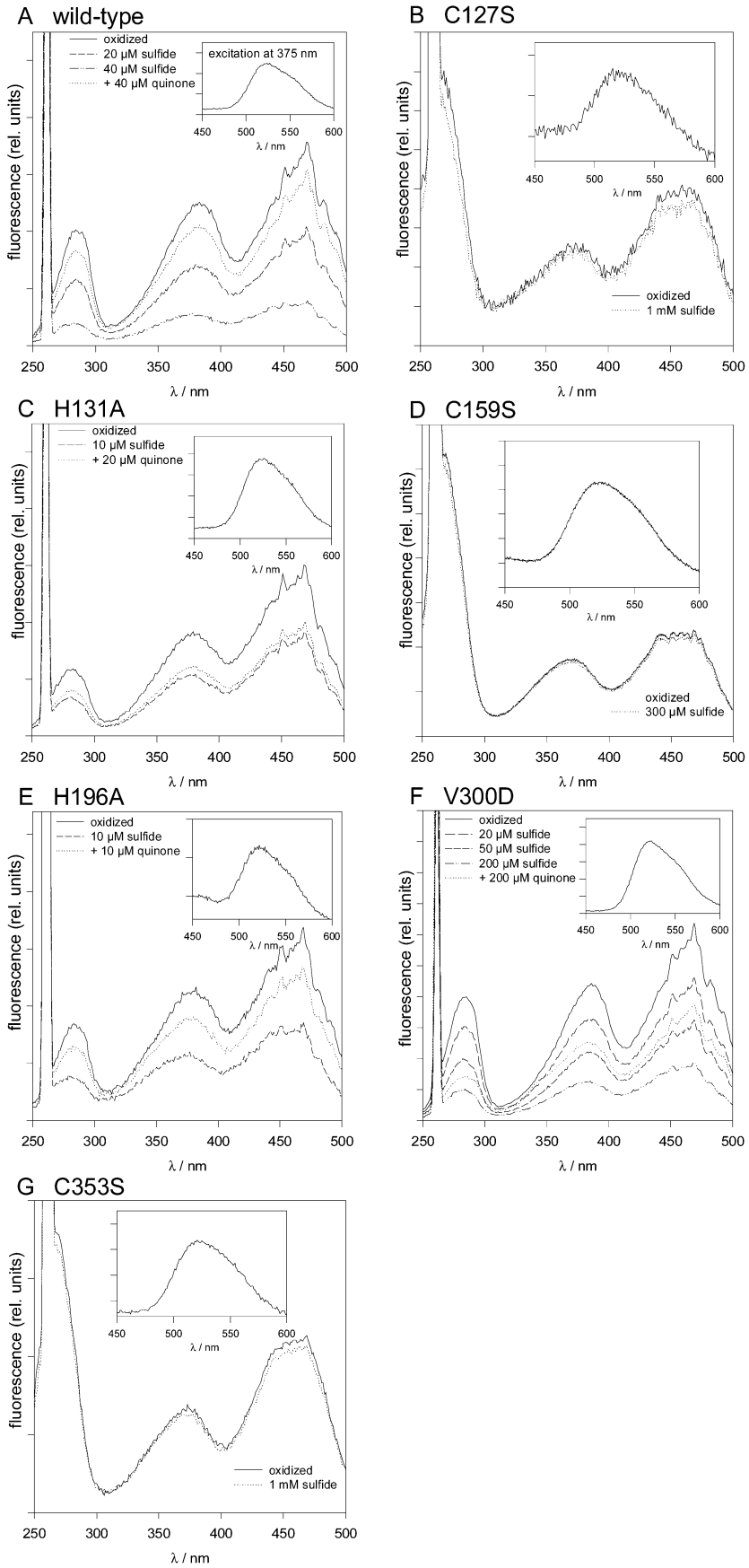

FIGURE 4: Fluorescence spectra of purified SQR. Excitation spectra (emission wavelength of 520 nm) were recorded before and after addition of different concentrations of sulfide. In panels B, D, and G, spectra were recorded 20 min after addition of sulfide. In panels A, E, and F, quinone was added at an equimolar concentration after reduction by sulfide. In panel C, the spectrum of the reoxidized SQR was recorded 15 min after addition of an excess amount of dUQ. Insets show emission spectra (excitation wavelength of 375 nm). The protein concentration was 0.2 mg/mL: (A) the wild type and (B−G) mutated enzymes.

below 300 nm, variability of the excitation spectra for different preparations of wild-type and mutated enzymes was observed. The reason for this variability is unknown so far. To determine which of the two half-reactions is inhibited in the mutated enzymes, sulfide was added. For none of the mutated enzymes could a sulfide-dependent fluorescence decrease be observed, even 20 min after addition of sulfide, indicating inhibition of the sulfide-dependent reduction of SQR.

V300D. Within the third FAD-binding domain, SQR is exceptional among the flavoprotein disulfide oxidoreductases because of the absence of a conserved aspartate that interacts with the ribityl chain of the flavin moiety of FAD (Figure 2E) (*10*). In SQR, there is a valine residue in this position (V300 in *Rb. capsulatus* SQR); the corresponding residue in SQR of *Thiobacillus ferrooxidans* is isoleucine. The absence of this aspartate in all SQRs is significant. Possibly, the conformation of FAD binding in SQR is somewhat different. Most interestingly, the HMT2 protein from *Schizosaccharomyces pombe*, which was postulated as the first eukaryotic SQR, possesses an aspartate residue in this position (*20*). The enzyme exhibits SQR activity, but the apparent K_m values for sulfide and quinone are both 2 mM; on the other hand, the values of all tested SQRs are in the micromolar range. Thus, the physiological role of HMT2 as a sulfide-quinone reductase is questionable. To analyze the difference between the valine and the aspartate in this position, V300 was mutated to aspartate.

The specific activity of His-SQR-V300D was ~6 units/mg, which is ~11% of that of the wild type (Table 1). The K_m for dUQ, determined in the presence of 400 μM sulfide (Figure 5), was 28 μM, which is ~1 order of magnitude higher than that of the wild type. For the measurement of the K_m for sulfide, there was the complication that dUQ could be tested in the SQR activity assay up to only 40 μM because of the low solubility in aqueous solution. With a K_m for dUQ of 28 μM, the measurement of the K_m for sulfide at 40 μM dUQ was performed under nonsaturating conditions of quinone. Even under quinone limitation, the determined K_m for sulfide of 400 μM (Figure 5) is 2 orders of magnitude higher than that of the wild-type enzyme. Since both K_m values have been determined under nonsaturating conditions for the second substrate, the real values are even higher. Anyway, a drastic decrease in the affinity for both substrates could be observed.

The fluorescence excitation and emission spectra were identical to those of the wild-type enzyme (Figure 4). Reduction of the enzyme by sulfide was achieved only at concentrations of ~200 μM, and reoxidation occurred with equimolar amounts of dUQ.

H131A and H196A. As discussed below, Rich and Fisher postulated a structural element for quinone-binding sites (*31*). Accordingly, two putative quinone binding peptides in SQR can be found around H131 and H196. H131 (*Rb. capsulatus*) is located in a putative α-helix formed by the conserved stretch [S-(I/V)-C-$(X)_3$-H-A-$(X)_2$-(A/T)] (Figure 2). H196 (*Rb. capsulatus*) is also located in a conserved stretch [E-P-Y-(V/I/L/A)-G-H-(L/M/F)-G-(L/I/V)]. Although the two regions are somewhat different from the proposed quinone-binding motifs, they were considered good candidates for the quinone-binding site in SQR; especially the aliphatic and aromatic amino acid residues in the vicinity of H131 might participate in forming a hydrophic quinone-binding pocket. The histidines are completely conserved in all SQR sequences, but absent in FCC, which does not bind quinone. Both histidines were mutated to alanine individually.

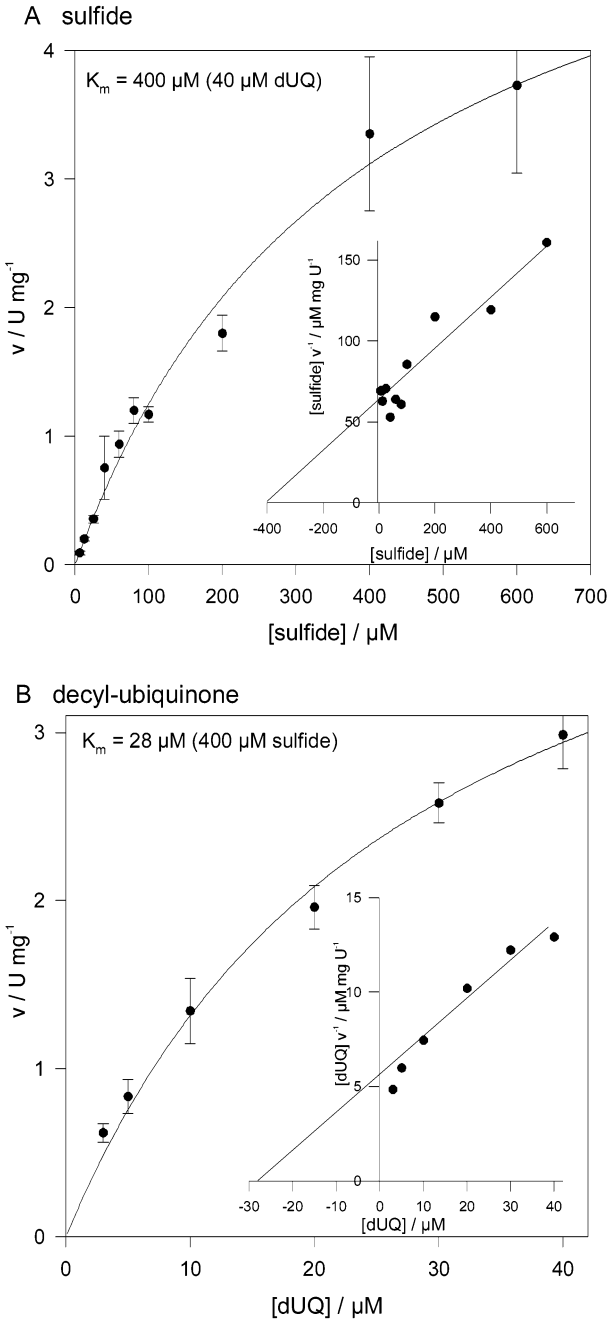

FIGURE 5: Substrate affinity of His-SQR-V300D. (A) K_m for sulfide was determined in the presence of a nonsaturating concentration of 40 μM dUQ, which is the highest measurable concentration. (B) K_m for dUQ with a constant concentration of 400 μM. As both determinations have been carried out under nonsaturating conditions of the other substrate, the real K_m values are even higher.

According to the proposed function of quinone binding, the mutation of at least one of the histidines to alanine was expected to result in a decrease in the affinity for quinone. However, there were no significant differences between the measured K_m values for dUQ of the mutated enzymes His-SQR-H131A and -H196A compared to the wild-type value of 3 μM (Table 1). The affinity of both enzymes for sulfide was slightly decreased, showing K_m values of 11 and 15 μM for H131A and H196A, respectively.

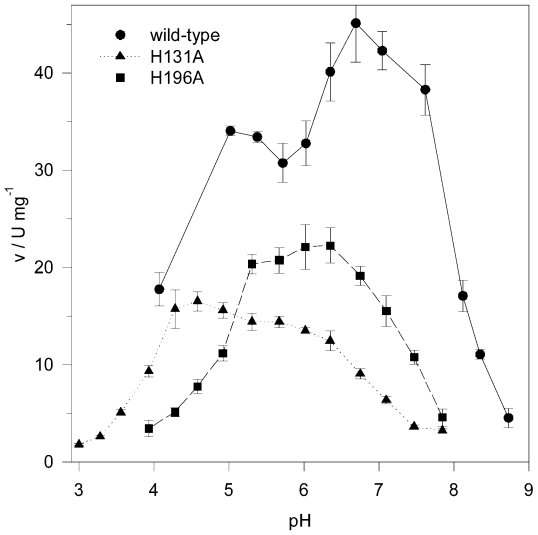

FIGURE 6: pH dependence of His-SQR activity for the wild type, H131A, and H196A.

Histidines exhibiting a p*K* of 6.5 in isolated form often take part in protonation reactions during enzymatic catalysis [e.g., within the glutathione reductase family (*14*)]. Therefore, mutations in histidines functioning as proton donors and acceptors should cause changes in the pH dependence of the activity. In Figure 6, the pH dependence of SQR activity is shown for the wild type, H131A, and H196A. Whereas the pH optimum of H196A was slightly shifted from 6.7 to 6.2, H131A showed a dramatic change in the pH dependence. The pH optimum was found to be ~4.5. As depicted in Figure 6, the specific activity was diminished for both mutated enzymes. For H131A, the specific activity was 20 and 27% of that of the wild-type enzyme at pH 6.5 and 4.5, respectively. The corresponding values for H196A were 38 and 40% at pH 6.5 and 6.2, respectively (Table 1).

The fluorescence excitation and emission spectra were identical to the wild-type spectra. Also, a sulfide-dependent decrease in the fluorescence intensity could be observed. However, there was no complete reoxidation by dUQ in the case of H131A even in the presence of an excess amount of quinone, indicating inhibition of the oxidative half-reaction (Figure 4).

Analysis of the Sulfur Product in the SQR Reaction

In contrast to many sulfide-oxidizing bacteria, which oxidize sulfide to sulfate, *Rb. capsulatus* oxidizes sulfide only to the level of elemental sulfur (*2*). Elemental sulfur is deposited as yellowish-white coating on cells growing on sulfide (Figure 3). At room temperature, elemental sulfur consists mainly of S_8 rings (*32*) and shows a very low solubility of 5 μg/L in aqueous solution (*33*). Since SQR is localized at the periplasmic side of the cytoplasmic membrane, the sulfur product of the SQR reaction has to be able to diffuse out of the periplasm. This is unlikely in the case of elemental sulfur because of its low solubility. Therefore, the primary product of the SQR reaction is most probably soluble polysulfide, which is in equilibrium with elemental sulfur (*34*). Formation of polysulfide after sulfide oxidation by SQR and deposition of elemental sulfur by growing cells is documented by the following experiments.

Stoichiometry of Sulfide and Quinone. To verify that sulfide is oxidized to the level of elemental sulfur by SQR in vitro, the stoichiometry of sulfide and quinone was determined. Under anaerobic conditions at pH 6.5, reduction of 40 μM dUQ by limiting amounts of sulfide was observed photometrically by measuring the absorption difference at 275 nm − 300 nm (for details, see SQR Activity Assay in Materials and Methods). Reduction of quinone was achieved with a nearly equimolar amount of sulfide (data not shown). In five experiments, 40 μM sulfide reduced 36.5 ± 0.7 μM dUQ on average.

Spectroscopic Analysis of Polysulfide. Absorption spectra of polysulfide solutions have been investigated by Klimmek et al. (*35*). A differential extinction coefficient $\epsilon_{360-550}$ of 0.36 mM^{-1} cm^{-1} at pH 8.5 was determined. At pH 8.0, the value was 0.38 mM^{-1} cm^{-1}. In our experiments, the polysulfide-specific absorption difference at 360 nm − 550 nm was recorded during sulfide-dependent reduction of quinone. The detergent Thesit was omitted in this assay, since there was no significant increase in absorption in its presence. At pH 6.5, 7.0, and 7.5, identical results were obtained. After subtraction of the baseline drift, there was a reproducible increase in absorption of 0.013 ± 0.002 during the reduction of 40 μM dUQ with 40 μM sulfide (data not shown). Using the extinction coefficient at pH 8.0 of 0.38 mM^{-1} cm^{-1}, this increase corresponds to a concentration of 34 μM polysulfide sulfur. In a control experiment, dUQ was reduced by $NaBH_4$. Thereby, no increase in the absorption difference at 360 nm − 550 nm was observed.

Use of $Na_2{}^{35}S$ as a Substrate. To trace the sulfur product of the SQR reaction, $Na_2{}^{35}S$ was used as a substrate for the isolated SQR. After the reaction, the amount of radioactivity bound to the SQR protein was determined to check the possibility of covalent binding of sulfur atoms to the enzyme during catalysis. Since H_2S is volatile and its first p*K* value is around 7.0, the experiments were performed at pH 8.0 to minimize the loss of $H_2{}^{35}S$ to the atmosphere. At this pH, SQR has 38% of its maximum activity (Figure 6).

The protein-bound proportion of radioactivity compared to the initial amount was in the range from 3.2 to 5.0% in all experiments (Table 2). Therefore, no specific increase in the amount of radioactivity during the SQR reaction could be observed. After SDS−PAGE, there was radioactivity bound to SQR under all conditions and to BSA, indicating nonspecific binding of sulfide to protein (not shown).

To determine if there any elemental sulfur could be detected under the conditions of the SQR assay, the experiments were modified as described in Materials and Methods. In all samples and controls, the proportion in the chloroform phase did not exceed 1.3%. This was taken as a hint that the primary product of the SQR reaction is not hydrophobic elemental sulfur, but water-soluble polysulfide.

HPLC Analysis of Sulfur Compounds. By using HPLC, different species of sulfur can be detected qualitatively and quantitatively (*30*). The pale yellow coating of *Rb. capsulatus* cells growing in the presence of sulfide (Figure 3) was investigated using HPLC. Analysis confirmed that it consists of elemental sulfur deposited outside the cells. Likewise, HPLC analysis was applied to the SQR reaction assay (see Materials and Methods) at pH 6.5 with the enzyme, buffer, 200 μM dUQ, and 200 μM sulfide. During the SQR reaction, samples were taken after 0, 1.5, 3, and 5 min. The results

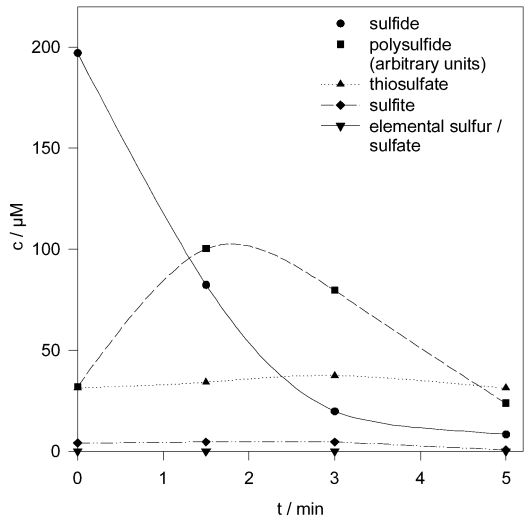

FIGURE 7: Analysis of sulfur compounds during the SQR reaction at pH 6.5 using HPLC. Reduction of 200 μM dUQ by SQR was started by addition of 200 μM sulfide. After 0, 1.5, 3, and 5 min, samples were taken and analyzed. Quantitation of polysulfide is not possible because of the variable chain length.

are shown in Figure 7. The concentration of sulfide decreased during the SQR reaction from 200 μM to zero. There was no evidence of the existence of elemental sulfur and sulfate. Furthermore, constant concentrations of thiosulfate and sulfite could be detected, which are usual contaminants in sulfide solutions (J. Rethmeier, personal communication). Most interestingly, the signal for polysulfide exhibited an intermediary increase during the reaction.

DISCUSSION

The sulfide-dependent reduction of quinone with sulfide by SQR (reaction 1) can be considered as the sum of two half-reactions: the sulfide-dependent reduction of the oxidized SQR (reaction 2) and the quinone-dependent reoxidation of the SQR (reaction 3).

$$H_2S + UQ \rightarrow [S^0] + UQH_2 \quad (1)$$

$$H_2S + E_{ox} \rightarrow [S^0] + EH_2 \quad (2)$$

$$EH_2 + UQ \rightarrow E_{ox} + UQH_2 \quad (3)$$

In the following, the primary oxidation product of sulfide is discussed, before the two half-reactions are described in detail.

Oxidation Product of Sulfide. In contrast to other sulfide-oxidizing bacteria, *Rb. capsulatus* oxidizes sulfide only to the level of elemental sulfur (*2*). This sulfur product is deposited as a pale yellow coating outside the cells, as shown in Figure 3. This coating was confirmed to be elemental sulfur by HPLC.

Since elemental sulfur, which consists at room temperature mainly of S_8 rings (*32*), is rather insoluble in aqueous solution with a solubility of 5 μg/L (*33*) and thus is unlikely to diffuse out of the periplasmic space, water-soluble polysulfide seems to be more likely to be the primary product of sulfide oxidation. Also, in experiments using isolated spheroplasts from *Chlorobium vibrioforme* and *Allochromatium minutissimum*, polysulfide has been detected as the product of sulfide oxidation, whereas with whole cells, elemental sulfur and thiosulfate have been found besides polysulfide (*36*). Obviously, the enzymes of isolated spheroplasts are able to oxidize sulfide to polysulfide. This finding is in agreement with our results about SQR as an enzyme bound to the periplasmic side of the cytoplasmic membrane.

The presence of polysulfide after the SQR reaction could be confirmed by using several independent experiments. The stoichiometry of sulfide and quinone indicated a sulfur product with an oxidation state slightly below S^0. The photometrical detection of polysulfide was complicated by the simultaneous reduction of dUQ absorbing in a similar range. After subtraction of the absorption change caused by the reduced dUQ, an increase in absorption of 0.013 ± 0.002 during the reduction of 40 μM dUQ with 40 μM sulfide at pH 7.5 was observed, which corresponds to a concentration of 34 μM polysulfide sulfur using an extinction coefficient of 0.38 mM^{-1} cm^{-1} at pH 8.0 (*35*). If we presume that pentasulfide is the predominant form of polysulfide according to Giggenbach (*37*), this absorption corresponds to an overall concentration of 42 μM sulfur atoms. In addition, HPLC analysis did not show any signal for elemental sulfur, but a transient signal for polysulfide (Figure 7), which is discussed below. Furthermore, after the reaction of SQR with $Na_2{}^{35}S$ and dUQ, there was no detectable radioactivity in the chloroform extraction, which would have been expected in the case of elemental sulfur as the primary product. Altogether, it is evident that polysulfide is the primary product of the SQR reaction.

However, what is the mechanism for the formation of polysulfide by SQR? In former discussions, it has been suggested that the polysulfide chain is built up bound to the enzyme (*12*). However, the presented results did not show any evidence of a sulfur product covalently bound to the enzyme. There was no specifically protein-bound radioactivity that could be detected after the reaction of SQR with $Na_2{}^{35}S$ and dUQ (Table 2). Taking this result together with the transient polysulfide signal from HPLC, the magnitude of which increases at the beginning of the reaction and decreases at the end (Figure 7), we propose another model for polysulfide formation now. Herein, disulfide is the initial product of sulfide oxidation, which is released from the enzyme. The postulated intermediary persulfide at one of the active site cysteines as depicted in state 3 of Scheme 1 seems to be unstable in the presence of excess amounts of sulfide. This intermediate does not appear to accumulate in large amounts, because no protein-bound radioactivity could be detected as described above. Most interestingly, the enzyme rhodanese, which catalyzes in vitro the transfer of a sulfane S atom from thiosulfate to the nucleophilic acceptor cyanide in a two-step reaction, forms a stable persulfide intermediate at a cysteine residue. This intermediate was even observed in the crystallized enzyme (*52*). However, in the case of SQR, the two steps cannot be separated, because HS^- is the substrate in both.

Polysulfide anions of different chain lengths are in equilibrium with each other (*34*, *37*). Therefore, longer-chain polysulfides can be formed by disproportionation reactions from the initial disulfide and the secondary formed trisulfide anions, which is shown in reactions 4 and 5. Since the concentration of sulfide is diminished by the SQR reaction, the equilibria of reactions 4 and 5 are shifted to the right.

Scheme 1: Proposed Mechanism of the Reductive Half-Reaction of SQR[a]

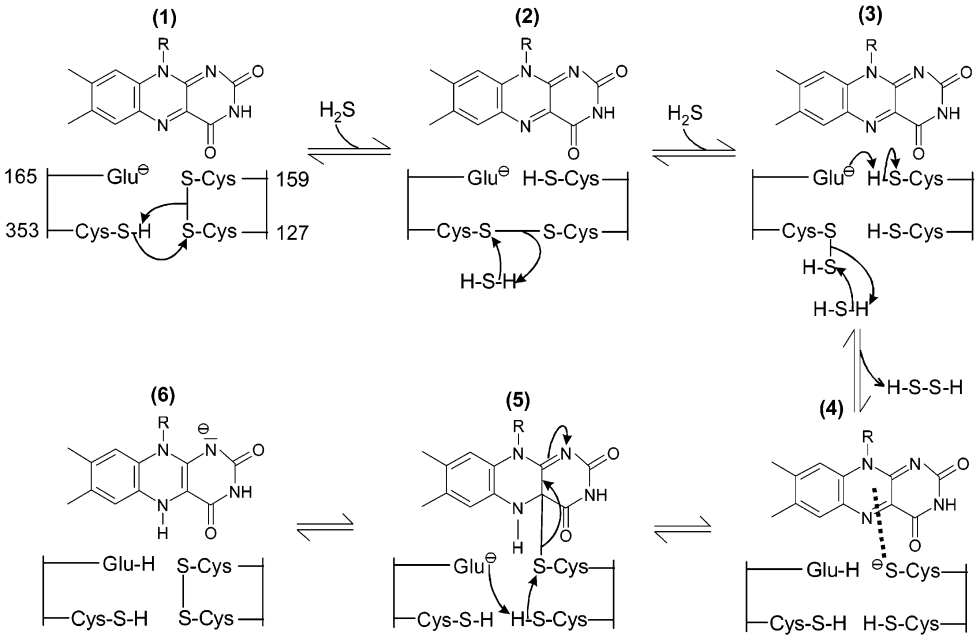

[a] The oxidized form of SQR (state 1) is in equilibrium with state 2 by disulfide exchange. Reaction with a sulfide molecule leads to a persulfide at C353 and a thiol at C127 (state 3). By nucleophilic attack of a second sulfide molecule on the persulfide, the thiol group at C353 is restored, and a free persulfide molecule as the primary product is released from the enzyme. The active site base E165 abstracts a proton from the thiol group of C159, leading to a charge transfer complex with the thiolate of C159 as the donor and the oxidized FAD as the acceptor, as depicted in state 4. Reduction of FAD occurs via a covalent adduct between flavin C(4a) and C159 (state 5), resulting in a reduced flavin and a disulfide bridge between C159 and C127 (state 6).

This increase in the average length of the formed polysulfide chains is indicated by the time course of HPLC analysis (Figure 7). Each polysulfide molecule reacts with two monobromobimane molecules at its ends, irrespective of the number of sulfur atoms in the chain. Thus, at the beginning of the reaction, when short-chain polysulfides prevail, the magnitude of the signal for polysulfide is high, but decreases later, when the chain length increases.

$$2\text{H-S-S}^- \rightleftharpoons \text{H-S-S-S}^- + \text{H-S}^- \quad (4)$$

$$2\text{H-S-S-S}^- \rightleftharpoons {}^-\text{S-(S)}_3\text{-S}^- + \text{H-S}^- + \text{H}^+ \quad (5)$$

The exact stoichiometry of sulfide and quinone in the SQR reaction was 1.1:1, indicating an average oxidation state of the sulfur product of -0.2 and thus polysulfide chains with an average chain length of 10 sulfur atoms at the end of the reaction. This is in contrast to measurements by Giggenbach (*37*), who investigated the distribution of various polysulfide species in aqueous solution. At neutral pH, he found mainly S_5^{2-} and S_4^{2-}.

Formation of elemental sulfur could be observed only during experiments with whole cells. With in vitro experiments that included SQR, buffer, detergent, dUQ, and sulfide, no elemental sulfur could be detected up to sulfide concentrations of 200 μM in a pH range from 6.5 to 8.0. The equilibrium between polysulfide and elemental sulfur is described by equation 6 (*34*).

$$\text{S}_n^{2-} + \text{H}^+ \rightleftharpoons \text{H-S}_n^- \rightleftharpoons \text{H-S}^- + \text{S}_{n-1} \quad (6)$$

Reductive Half-Reaction of SQR. Disulfide oxidoreductase flavoproteins catalyze the electron transfer between C and S centers (*14*, *15*), e.g., between dihydrolipoamide and NAD^+ in the case of lipoamide dehydrogenase. The physiological direction of electron transfer from the S to the C center in lipoamide dehydrogenase corresponds to that of SQR, which transfers electrons from sulfide to quinone. Sulfide-dependent reduction of the enzyme to the EH_2 state is the reductive half-reaction in the case of SQR and corresponds to the reductive half-reaction of lipoamide dehydrogenase, but to the oxidative half-reaction of glutathione reductase and thioredoxin reductase, which are oxidized by sulfur substrates.

In disulfide oxidoreductase flavoproteins, electron transfer between S centers and FAD occurs via a pair of cysteines, which change state between disulfide and dithiol. Within this reaction, each of the cysteines has a special function (*14*). One of the cysteines is more exposed and responsible for the interaction with the thiol substrate, and the other one is located closer to the flavin and performs the electron transfer with the isoalloxazine moiety. For lipoamide dehydrogenase, the specific roles of the two cysteine residues were established by directed mutagenesis (*38*). The general reaction between the enzyme (E) disulfide and the substrate (Sub) dithiol is shown in reactions 7 and 8. By reduction of the enzyme disulfide by a substrate dithiol, an intermediary mixed disulfide between the substrate and the exposed cysteine residue is formed (reaction 7). By a nucleophilic attack of the second thiol group of the substrate, the mixed disulfide is resolved, and an enzyme dithiol and a substrate disulfide are generated (*14*), as shown in reaction 8. The oxidized flavin is subsequently reduced by the enzyme dithiol. In addition to the redox active cysteine pair, a basic residue in the active site is important for catalysis within this flavoprotein family. By abstraction of a proton from the cysteine, the thiolate is formed, which is more nucleophilic

than the protonated form. This active site base is a histidine residue in glutathione reductase (*39*) and lipoamide dehydrogenase (*14*) and an aspartate in the case of thioredoxin reductase (*40*). The importance of the active site base was demonstrated for lipoamide dehydrogenase by site-directed mutagenesis. Replacement of this histidine with glutamine led to a drastic decrease in the activity and the loss of charge transfer absorption (*14*). In the case of flavocytochrome *c*, the mechanism has not been studied at this level of detail, but in measurements with adducts between sulfite and flavin, a base in the active site was observed, with a p*K* value of 6.5. Thus, this active site base was first assumed to be a histidine (*8*), but after the determination of the FCC structure turned out to be a glutamate (*9*).

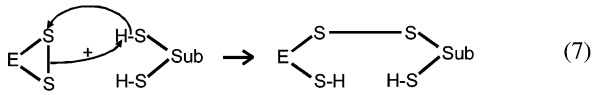

(7)

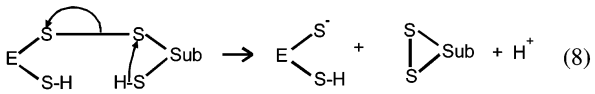

(8)

Since the mechanism of electron transfer between dithiol substrates and flavin is conserved within the disulfide oxidoreductase flavoproteins, the same mechanism could hold for SQR. There are three conserved cysteine residues in SQR. Mutation of each of them to serine leads to nearly complete inactivation of the enzyme, indicating a special function for each of the three cysteines, which cannot be performed by the other two. The finding that the flavin fluorescence is not decreased by sulfide in any of these mutated enzymes is an indication of the involvement of all three cysteine residues in the reductive half-reaction. Two of the cysteines (C159 and C353 in *Rb. capsulatus* SQR) are located at identical positions in the sequence as the cysteines forming the redox active disulfide bridge in FCC (Figure 2). However, there is a third conserved cysteine (C127), the mutation to serine of which also resulted in nearly complete inactivation of the enzyme. Fluorescence measurements revealed inhibition of the reductive half-reaction. Therefore, our proposal for the reaction mechanism must also include C127 (Scheme 1), although models for a mechanism including only two cysteine residues are conceivable. Perhaps the third cysteine makes up for the second sulfur atom missing in sulfide in comparison to the substrates for other members in the disulfide oxidoreductase family, like lipoamide, glutathione, or thioredoxin (*14*). As the apparent K_m value for sulfide of His-SQR-C127S was nearly identical to the value found for the wild-type enzyme, C127 is not supposed to interact directly with the sulfide substrate, but to be involved in the reductive half-reaction as part of a disulfide bridge. Therefore, in the mechanism that we propose for SQR, the redox active disulfide bridge is formed by C127 and C159, whereas C353 interacts with the sulfide substrate. For refinement of the model, further investigation is necessary, e.g., chemical modification of cysteine residues under different conditions. Furthermore, the crystal structure of SQR would provide a better understanding of the different functions of the cysteines. The low but measurable remaining activities of the three mutated enzymes cannot be explained on the basis of the proposed model. Possibly, sulfide-dependent reduction of quinone in the mutated enzymes takes place without the involvement of FAD in a bypass reaction. The active site base in this model is E165, which is homologous to the active site base (E167) in flavocytochrome *c*. Investigations about the function of E165 in SQR are in progress.

The oxidized form of SQR is represented by state 1 in Scheme 1. It is in equilibrium with state 2 by disulfide exchange. After reduction by a sulfide molecule, a persulfide at C353 and a thiol at C127 are formed (state 3). By nucleophilic attack of a second sulfide molecule on the persulfide, the thiol group at C353 is restored, and a free persulfide molecule as a primary product is released from the enzyme. The following steps are conserved in disulfide oxidoreductase flavoproteins and should also occur in SQR. The active site base E165 abstracts a proton from the thiol group of C159, leading to a charge transfer complex with the thiolate of C159 as the donor and the oxidized FAD as the acceptor, as depicted in state 4. Reduction of FAD occurs via a covalent adduct between flavin C(4a) and C159 (state 5), resulting in a reduced flavin and a disulfide bridge between C159 and C127 (state 6). Experiments for investigating the postulated charge transfer complex and the covalent C(4a) adduct are currently in progress.

In the context of the reductive half-reaction, the function of V300 has to be considered. SQR differs from other members of the glutathione reductase family in the absence of an aspartate residue within the third FAD-binding domain. At this position, there is a valine (isoleucine in the SQR of *T. ferrooxidans*). HMT2 from *S. pombe* has been postulated as the first eukaryotic SQR (*20*). This enzyme, which has an aspartate residue at the corresponding position, exhibits SQR activity in vitro, but has a very low affinity for both substrates. The K_m values are 2 mM for sulfide as well as for quinone, whereas all SQRs exhibit K_m values in the micromolar range (*12*). Indeed, in SQR, the exchange of V300 against aspartate significantly lowers the affinities for both substrates (Figure 5). However, although the low affinity of SQR-V300D for sulfide is consistent with the high K_m of HMT2, it is in contrast to FCC, which contains an aspartate at the corresponding position, but with 12.5 μM has a low K_m for sulfide (*41*). The decrease in the affinity in SQR-V300D could be related to the introduction of a negative charge close to the flavin. Possibly the redox potential of the flavin is lowered unfavorably (*42*), which has to be tested by measurement of the midpoint potential of wild-type SQR and SQR-V300D. Alternatively, the negative charge of the aspartate could be close to the binding site for sulfide, causing repulsion of this anionic substrate.

Oxidative Half-Reaction of SQR. The oxidative half-reaction of SQR is represented by the quinone-dependent reoxidation of the reduced enzyme, as described in reaction 3. On the basis of crystallographic data of several quinone-binding proteins, Rich and Fisher proposed a structural element for quinone-binding sites (*31*). It is composed of a helical stretch that flanks one side of the quinone headgroup and contains a triad of close contact residues. The central residue of the triad is a histidine which forms a hydrogen bond to one carbonyl of the quinone. The fourth residue upstream of this histidine is aliphatic, usually leucine, and is the closest of the triad to the isoprenoid side chain. Another close contact residue three or four residues downstream, the

Scheme 2: Proposed Mechanism of the Oxidative Half-Reaction of SQR[a]

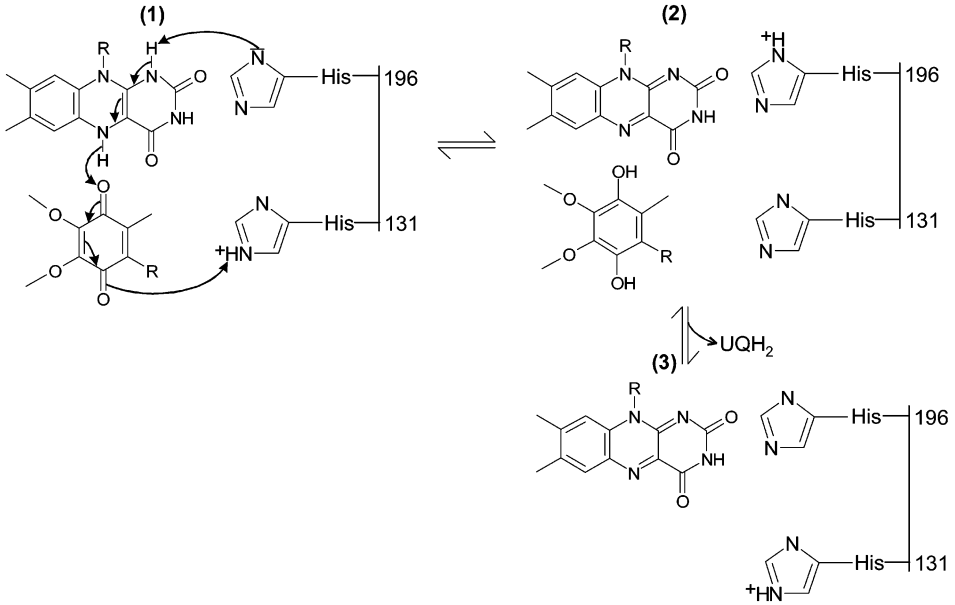

[a] In a concerted reaction, hydride transfer from flavin atom N(5) to dUQ occurs, accompanied by the transfer of the proton from flavin N(1) to the deprotonated H196, and protonation of the second carbonyl group of dUQ from H131 takes place, which is in the proximity of the bound dUQ (state 1). In state 2, the reduced dUQ ($dUQH_2$) and the oxidized flavin are depicted. Reprotonation of H131 by H196 leads to the original oxidized state of the enzyme (state 3).

histidine makes up the contact triad and is well-conserved within homologous sequences of different Q-binding proteins.

As a model flavoprotein for the oxidative half-reaction, NAD(P)H:quinone oxidoreductase (DT-diaphorase) was used for a mechanistic comparison, which catalyzes the NAD(P)H-dependent reduction of quinone (*43*). During this reaction, base-catalyzed hydride transfer between NAD(P)H and FAD and between $FADH_2$ and quinone occurs (*44*). On the basis of structural data, a tyrosine and a histidine residue were presumed as active site bases. Whereas replacement of the histidine residue with glutamine resulted in an enzyme with an activity of only 8% of that of the wild type, mutagenesis of the tyrosine led to a smaller loss of activity to 35% (*45*, *46*). Thus, the involvement of this tyrosine is questionable.

When the model of Rich and Fisher (*31*) is considered, one of the two conserved histidines in SQR could be involved in the binding of quinone. In this case, the affinity for quinone should drop after the mutation to alanine. However, for none of the two mutated enzymes could an increase in the K_m be observed. Other possible roles in catalysis for histidine residues are protonation or deprotonation reactions. This function could be investigated by measuring the pH dependence of the reaction. The wild-type enzyme exhibits a pH optimum at pH 6.7 and a smaller optimum in the range of pH 5.0, indicating two different mechanisms of protonation of an intermediate. His-SQR-H131A shows a drastic decrease in activity to 20% of that of the wild type and the loss of the pH optimum in the range of pH 6.7. However, there is an activity peak at pH ~4.5 (Figure 6). This observation leads to the conclusion that in the acidic range the protonation occurs with protons from the environment, whereas H131 performs the protonation in the neutral range. The latter mechanism is obviously inhibited in His-SQR-H131A. The involvement of this residue in the oxidative half-reaction can be concluded from the observation that in His-SQR-H131A reoxidation does not occur completely even in the presence of a small excess of dUQ, which could be observed in the fluorescence experiment (Figure 4). If H131 is the proton donor in the oxidative half-reaction, protonation of dUQ as depicted in Scheme 2 is rate-limiting in the neutral range, leading to a smaller observable turnover, whereas in the acidic range, protonation can occur with protons from the environment. The fact that in His-SQR-H131A at pH 4.5 activity is not 100% of wild-type activity is probably due to an unfavorable effect of the acidic pH on other parts of the enzyme reaction. However, the lack of complete reoxidation of His-SQR-H131A by dUQ cannot be explained by kinetic effects, because the fluorescence experiment was carried out under equilibrium conditions. The mutation obviously also causes a thermodynamic effect. There are several conceivable explanations for the lack of reoxidation. The redox potential of the enzyme-bound FAD has possibly been shifted to more positive values by the H131A mutation. This has to be measured. Another explanation for the lack of reoxidation of $FADH_2$ by dUQ could be a selectively stronger binding of $dUQH_2$ to the active site, while the affinity for dUQ remains unchanged, as has been determined. H196 seems to be of less importance. The specific activity of His-SQR-H196A is 38% of that of the wild type. The slight shift of the pH optimum from 6.7 to 6.2 indicates the involvement of H196 in a protonation reaction as well.

In Scheme 2, a possible mechanism for the oxidative half-reaction with participation of H131 and H196 is depicted, taking only the kinetic effect of the mutation H131A into consideration. In the first step, the protonated H131 is in the proximity of the bound dUQ. The carbonyl group of dUQ can perform an attack on the proton. Below pH 5.0, dUQ can be protonated by protons from the environment. After the protonation, hydride transfer from flavin atom N(5) to dUQ can occur and be accompanied by the transfer of the proton from flavin N(1) to the deprotonated H196. In state

2, the reduced dUQ ($dUQH_2$) and the oxidized flavin are depicted. Reprotonation of H131 by H196 leads to the original oxidized state of the enzyme, as shown in state 3.

This model takes the different levels of importance of H131 and H196 into account. The reoxidation of the reduced flavin is initiated by the protonation of the oxidized dUQ by H131. Thus, the mutation H131A has a more significant effect on the activity of the enzyme. The function of H196 is deprotonation of flavin N(1) and reprotonation of H131, which is of less importance for the oxidative half-reaction and is reflected by the less drastic effect of the H196A mutation. The reprotonation can also be carried out by protons from the environment below pH 6.2, which can be concluded from the slight shift in the optimum of His-SQR-H196A from pH 6.7 to 6.2. If in His-SQR-H196A the reprotonation of H131 is rate-limiting, for the whole reaction, the p*K* of H131 can be calculated from the right slope of the pH curve of His-SQR-H196A. The half-maximum activity of this enzyme was observed at pH 7.1, which should be the p*K* of H131 according to this model.

ACKNOWLEDGMENT

We thank Jörg Rethmeier and Ulrich Fischer (Marine Mikrobiologie, Universität Bremen, Bremen, Germany) for HPLC analysis of the sulfur product. We thank Achim Kröger (Institut für Mikrobiologie, Johann Wolfgang Goethe-Universität Frankfurt am Main, Frankfurt am Main, Germany) and Ralf Steudel (Institut für Anorganische und Analytische Chemie, Technische Universität Berlin, Berlin, Germany) for helpful discussion about the chemistry of polysulfides and sulfur.

REFERENCES

1. Friedrich, C. G. (1998) Physiology and genetics of bacterial sulfur oxidation, in *Advances in microbial physiology* (Poole, R. K., Ed.) pp 236−289, Academic Press, London.
2. Hansen, T. A., and Van Gemerden, H. (1972) Sulfide utilization by purple nonsulfur bacteria, *Arch. Microbiol. 86*, 49−56.
3. Brune, D. C. (1995) Sulfur compounds as photosynthetic electron donors, in *Anoxygenic photosynthetic bacteria* (Blankenship, R. E., Madigan, M. T., and Bauer, C. E., Eds.) pp 847−870, Kluwer, Dordrecht, Netherlands.
4. Meyer, T. E., and Bartsch, R. G. (1976) The reaction of flavocytochromes *c* of the phototrophic sulfur bacteria with thiosulfate, sulfite, cyanide and mercaptans, in *Flavins and Flavoproteins* (Singer, T. P., Ed.) pp 312−317, Elsevier, Amsterdam.
5. Tollin, G., Meyer, T. E., and Cusanovich, M. A. (1982) Intramolecular electron transfer in *Chlorobium thiosulfatophilum* flavocytochrome *c*, *Biochemistry 21*, 3849−3856.
6. Cusanovich, M. A., Meyer, T. E., and Tollin, G. (1985) Flavocytochrome *c* transient kinetics of photoreduction by flavin analogs, *Biochemistry 24*, 1281−1287.
7. Guo, L. H., Hill, H.-A. O., Hopper, D. J., Lawrence, G. A., and Sanghera, G. S. (1990) Direct voltammetry of the chromatium-vinosum enzyme sulfide cytochrome *c* oxidoreductase flavocytochrome *c*-552, *J. Biol. Chem. 265*, 1958−1963.
8. Meyer, T. E., Bartsch, R. G., and Cusanovich, M. A. (1991) Adduct Formation between Sulfite and Flavin of Phototrophic Bacterial Flavocytochromes *c*. Kinetics of Sequential Bleach, Recolor, and Rebleach of Flavin as a Function of pH, *Biochemistry 30*, 8840−8845.
9. Chen, Z. W., Koh, M., Van Driessche, G., Van Beeumen, J. J., Bartsch, R. G., Meyer, T. E., Cusanovich, M. A., and Mathews, F. S. (1994) The Structure of Flavocytochrome *c* Sulfide Dehydrogenase from a Purple Phototrophic Bacterium, *Science 266*, 430−432.
10. Van Driessche, G., Koh, M., Chen, Z. W., Mathews, F. S., Meyer, T. E., Bartsch, R. G., Cusanovich, M. A., and Van Beeumen, J. J. (1996) Covalent structure of the flavoprotein subunit of the flavocytochrome *c*: Sulfide dehydrogenase from the purple phototrophic bacterium *Chromatium vinosum*, *Protein Sci. 5*, 1753−1764.
11. Reinartz, M., Tschaepe, J., Brueser, T., Trueper, H. G., and Dahl, C. (1998) Sulfide oxidation in the phototrophic sulfur bacterium *Chromatium vinosum*, *Arch. Microbiol. 170*, 59−68.
12. Griesbeck, C., Hauska, G., and Schütz, M. (2000) Biological Sulfide Oxidation: Sulfide-Quinone-Reductase (SQR), the Primary Reaction, in *Recent Research Developments in Microbiology* (Pandalai, S. G., Ed.) Vol. 4, pp 179−203, Research Signpost, Trivandrum, India.
13. Schütz, M., Maldener, I., Griesbeck, C., and Hauska, G. (1999) Sulfide-Quinone Reductase from *Rhodobacter capsulatus*: Requirement for Growth, Periplasmic Localization and Extension of Gene Sequence Analysis, *J. Bacteriol. 181*, 6516−6523.
14. Williams, C. H., Jr. (1992) Lipoamide Dehydrogenase, Glutathione Reductase, Thioredoxin Reductase, And Mercuric Ion Reductase: A Family Of Flavoenzyme Transhydrogenases, in *Chemistry and Biochemistry of Flavoenzymes* (Müller, F., Ed.) Vol. III, pp 121−211, CRC Press, Boca Raton, FL.
15. Massey, V., and Hemmerich, P. (1980) Active-site probes of flavoproteins, *Biochem. Soc. Trans. 8*, 246−257.
16. Grieshaber, M. K., and Völkel, S. (1998) Animal adaptions for tolerance and exploitation of poisonous sulfide, *Annu. Rev. Physiol. 60*, 33−53.
17. Parrino, V., Kraus, D. W., and Doeller, J. E. (2000) ATP production from the oxidation of sulfide in gill mitochondria of the ribbed mussel *Geukensia demissa*, *J. Exp. Biol. 203*, 2209−2218.
18. Yong, R., and Searcy, D. G. (2001) Sulfide oxidation coupled to ATP synthesis in chicken liver mitochondria, *Comp. Biochem. Physiol., Part B: Biochem. Mol. Biol. 129*, 129−137.
19. Furne, J., Springfield, J., Koenig, T., DeMaster, E., and Levitt, M. D. (2001) Oxidation of hydrogen sulfide and methanethiol to thiosulfate by rat tissues: a specialized function of the colonic mucosa, *Biochem. Pharmacol. 62*, 255−259.
20. Vande Weghe, J. G., and Ow, D. W. (1999) A Fission Yeast Gene for Mitochondrial Sulfide Oxidation, *J. Biol. Chem. 274*, 13250−13257.
21. Grant, S., Jersee, J., Bloom, F., and Hanahan, D. (1990) Differential plasmid rescue from transgenic mouse DNAs into *Escherichia coli* methylation-restriction mutants, *Proc. Natl. Acad. Sci. U.S.A. 87*, 4645−4649.
22. Studier, F. W., Rosenberg, A. H., Dunn, J. J., and Dubendorff, J. W. (1990) Use of T7 RNA polymerase to direct expression of cloned genes, *Methods Enzymol. 185*, 60−98.
23. Maniatis, T., Fritsch, E. F., and Sambrook, J. (1989) *Molecular cloning: a laboratory manual*, Cold Spring Harbor Laboratory Press, Plainview, NY.
24. Schütz, M., Shahak, Y., Padan, E., and Hauska, G. (1997) Sulfide-quinone reductase from *Rhodobacter capsulatus*: Purification, cloning and expression, *J. Biol. Chem. 272*, 9890−9894.
25. Tabor, S., and Richardson, C. C. (1985) A bacteriophage T-7 RNA polymerase-promotor system for controlled exclusive expression of specific genes, *Proc. Natl. Acad. Sci. U.S.A. 82*, 1074−1078.
26. Shahak, Y., Klughammer, C., Padan, E., Herrmann, I., and Hauska, G. (1994) Sulfide-quinone and sulfide-cytochrome reduction in *Rhodobacter capsulatus*, *Photosynth. Res. 39*, 175−181.
27. Morton, R. A. (1965) Spectroscopy of quinones and related substances, in *Biochemistry of quinones* (Morton, R. A., Ed.) pp 23−64, Academic Press, London.
28. Laemmli, U. K. (1970) Cleavage of structural proteins during the assembly of the head of bacteriophage T4, *Nature 227*, 680−685.
29. Trüper, H. G., and Schlegel, H. G. (1964) Sulphur metabolism in *Thiorhodaceae*. 1. Quantitative measurements on growing cells of *Chromatium okenii*, *Antonie van Leeuwenhoek 30*, 225−238.
30. Rethmeier, J., Rabenstein, A., Langer, M., and Fischer, U. (1997) Detection of traces of oxidized and reduced sulfur compounds in small samples by combination of different high-performance liquid chromatography methods, *J. Chromatogr., A 760*, 295−302.
31. Rich, P., and Fisher, N. (1999) Quinone-Binding Sites in Membrane Proteins: Structure, Function and Applied Aspects, *Biochem. Soc. Trans. 27*, 561−565.
32. Steudel, R. (1996) Das gelbe Element und seine erstaunliche Vielseitigkeit, *Chem. Unserer Zeit 30*, 226−234.
33. Boulégue, J. (1978) Solubility of elemental sulfur in water at 298 K, *Phosphorus Sulfur Relat. Elem. 5*, 127−128.

34. Steudel, R. (1996) Mechanism for the Formation of Elemental Sulfur from Aqueous Sulfide in Chemical and Microbiological Desulfurization Processes, *Ind. Eng. Chem. Res. 35*, 1417−1423.
35. Klimmek, O., Kröger, A., Steudel, R., and Holdt, G. (1991) Growth of *Wolinella succinogenes* with polysulfide as terminal acceptor of phosphorylative electron transport, *Arch. Microbiol. 155*, 177−182.
36. Blöthe, M., and Fischer, U. (2000) New insights in sulfur metabolism of purple and green phototrophic sulfur bacteria and their spheroblasts, in *BIOspektrum, Sonderausgabe zum 1. Gemeinsamen Kongress der DGHM, ÖGHMP und VAAM: "Microbiology 2000" vom 12. bis 16. März 2000 in München* (Heesemann, J., Ed.) p 62, Spektrum Akademischer Verlag, Heidelberg, Germany.
37. Giggenbach, W. (1972) Optical Spectra and Equilibrium Distribution of Polysulfide Ions in Aqueous Solution at 20 °C, *Inorg. Chem. 11*, 1201−1207.
38. Hopkins, N., and Williams, C. H., Jr. (1995) Characterization of Lipoamide Dehydrogenase from *Escherichia coli* Lacking the Redox Active Disulfide: C44S and C49S, *Biochemistry 34*, 11757−11765.
39. Pai, E. F., and Schulz, G. E. (1983) The Catalytic Mechanism of Glutathione Reductase as Derived from X-ray Diffraction Analyses of Reaction Intermediates, *J. Biol. Chem. 258*, 1752−1757.
40. Williams, C. H., Jr. (1995) Mechanism and structure of thioredoxin reductase from *Escherichia coli*, *FASEB J. 9*, 1267−1276.
41. Cusanovich, M. A., Meyer, T. E., and Bartsch, R. G. (1991) Flavocytochrome *c*, in *Chemistry and Biochemistry of Flavoenzymes* (Müller, F., Ed.) Vol. II, pp 377−393, CRC Press, Boca Raton, FL.
42. Ghisla, S., and Massey, V. (1989) Mechanisms of flavoprotein-catalyzed reactions, *Eur. J. Biochem. 181*, 1−17.
43. Tedeschi, G., Chen, S., and Massey, V. (1995) DT-Diaphorase. Redox Potential, Steady-State, and Rapid Reaction Studies, *J. Biol. Chem. 270*, 1198−1204.
44. Li, R., Bianchet, M. A., Talalay, P., and Amzel, L. M. (1995) The three-dimensional structure of NAD(P)H:quinone reductase, a flavoprotein involved in cancer chemoprotection and chemotherapy: Mechanism of the two-electron reduction, *Proc. Natl. Acad. Sci. U.S.A. 92*, 8846−8850.
45. Chen, S., Wu, K., Zhang, D., Sherman, M., Knox, R., and Yang, C. S. (1999) Molecular characterization of binding of substrates and inhibitors to DT-diaphorase: combined approach involving site-directed mutagenesis, inhibitor-binding analysis, and computer modeling, *Mol. Pharmacol. 56*, 272−278.
46. Chen, S., Wu, K., and Knox, R. (2000) Structure−Function Studies of DT-Diaphorase (NQO1) and NRH:Quinone Oxidoreductase (NQO2), *Free Radical Biol. Med. 29*, 276−284.
47. Bronstein, M., Schütz, M., Hauska, G., Padan, E., and Shahak, Y. (2000) Cyanobacterial sulfide-quinone reductase (SQR): cloning and heterologous expression, *J. Bacteriol. 182*, 3336−3344.
48. Nübel, T., Klughammer, C., Huber, R., Hauska, G., and Schütz, M. (2000) Sulfide-quinone reductase in membranes of the hyperthermophilic bacterium *Aquifex aeolicus* VF5, *Arch. Microbiol. 173*, 233−244.
49. Deckert, G., Warren, P. V., Gaasterland, T., Young, W. G., Lenox, A. L., Graham, D. E., Overbeek, R., Snead, M. A., Keller, M., Aujay, M., Huber, R., Feldman, R. A., Short, J. M., Olsen, G. J., and Swanson, R. V. (1998) The complete genome of the hyperthermophilic bacterium *Aquifex aeolicus*, *Nature 392*, 353−358.
50. Krauth-Siegel, R. L., Blatterspiel, R., Saleh, M., Schiltz, E., Schirmer, R. H., and Untucht-Grau, R. (1982) Glutathione reductase from human erythrocytes. The sequences of the NADPH domain and of the interface domain, *Eur. J. Biochem. 12*, 259−267.
51. Westphal, A. H., and deKok, A. (1988) Lipoamide dehydrogenase from *Azotobacter vinelandii*. Molecular cloning, organization and sequence analysis of the gene, *Eur. J. Biochem. 172*, 299−305.
52. Gliubich, F., Berni, R., Colapietro, M., Barba, L., and Zanotti, G. (1998) Structure of Sulfur-Substituted Rhodanese at 1.36 Å Resolution, *Acta Crystallogr. D54*, 481−486.

BI026032B